NANO LETTERS

2007
Vol. 7, No. 11
3315−3319

Directed Growth of Horizontally Aligned Gallium Nitride Nanowires for Nanoelectromechanical Resonator Arrays

Tania Henry, Kyungkon Kim, Zaiyuan Ren, Christopher Yerino, and Jung Han*

Department of Electrical Engineering, Yale University, New Haven, Connecticut 06520

Hong X. Tang*

Departments of Electrical Engineering and Mechanical Engineering, Yale University, New Haven, Connecticut 06520

Received June 27, 2007; Revised Manuscript Received September 8, 2007

ABSTRACT

We report the growth of horizontally aligned arrays and networks of GaN nanowires (NWs) as resonant components in nanoelectromechanical systems (NEMS). A combination of top-down selective area growth (SAG) and bottom-up vapor–liquid–solid (VLS) synthesis enables flexible fabrication of highly ordered nanowire arrays in situ with no postgrowth dispersion. Mechanical resonance of free-standing nanowires are measured, with quality factors (*Q*) ranging from 400 to 1000. We obtained a Young's modulus (*E*) of ~338 GPa from an array of NWs with varying diameters and lengths. The measurement allows detection of nanowire motion with a rotating frame and reveals dual fundamental resonant modes in two orthogonal planes. A universal ratio between the resonant frequencies of these two fundamental modes, irrespective of their dimensions, is observed and attributed to an isosceles cross section of GaN NWs.

Recent studies on semiconducting nanowire (NW) structures have focused primarily on exploring a nanowire's electronic and photonic properties.[1,2] Most NWs are prepared by the catalytic vapor−liquid−solid (VLS) method on amorphous or polycrystalline substrates. The as-grown, haystacklike NWs are transferred through solution sonication and dispersed randomly onto target wafers, where electrical contacting and/or characterization are subsequently performed.

Because of their extremely light weight (on the order of femtograms), nanowires also offer unique opportunities as mechanical resonators in pushing the sensitivity of mass detection beyond zeptogram ($<10^{-21}$ g) level.[3−5] In the pursuit of ever-decreasing cross section and weight of resonators, nearly all the nanoelectromechanical system (NEMS) sensing devices have relied on top-down electron-beam lithography.[6] Significant challenges exist, however, despite the impressive progress made in recent years, in continuing the trend of top-down sculpting of NEMS devices: (i) dimensional control at the nanometer scale, (ii) process (etching) induced surface damages and roughness, (iii) structural damages during the last step of selective etching of the sacrificial layer (release), (iv) a tendency of degradation of electronic properties, and (v) a systematic decrease in quality factor (Q) for the resonators.[7]

The purpose of this paper is to demonstrate a hybrid approach toward the construction of NW arrays and networks through the use of (optical) lithographically defined selective-area growth (SAG) in conjunction with bottom-up VLS synthesis of epitaxially aligned NWs in order to alleviate the burden associated with nanoscale fabrication. Spatially aligned and flexibly patterned NW networks are prepared in which the stochastic nature in contemporary process of NW synthesis and fabrication is greatly mitigated. While we anticipate new opportunities rendered by this novel and more deterministic fabrication process in pursuing NW-based electronic and photonic applications, we will focus in this report on the nanomechanical characterization of ordered NW arrays to demonstrate the possibility of a new direction in NW research that is orthogonal yet complementary to existing nanoelectronic and nanophotonic studies.

The synthesis starts with MOCVD growth of GaN (or AlN) buffer on sapphire substrate. The choice of AlN buffers would allow electrical insulation among GaN SAG mesas (Figure 1a). All MOCVD processes in this work were carried out in a commercial horizontal reactor (Aixtron 200/4 HT-S).[8] Trimethylgallium (TMGa), trimethylaluminum (TMAl),

* Corresponding authors. E-mail: jung.han@yale.edu (J.H.); hong.tang@yale.edu (H.X.T.).

10.1021/nl071530x CCC: $37.00 © 2007 American Chemical Society
Published on Web 10/17/2007

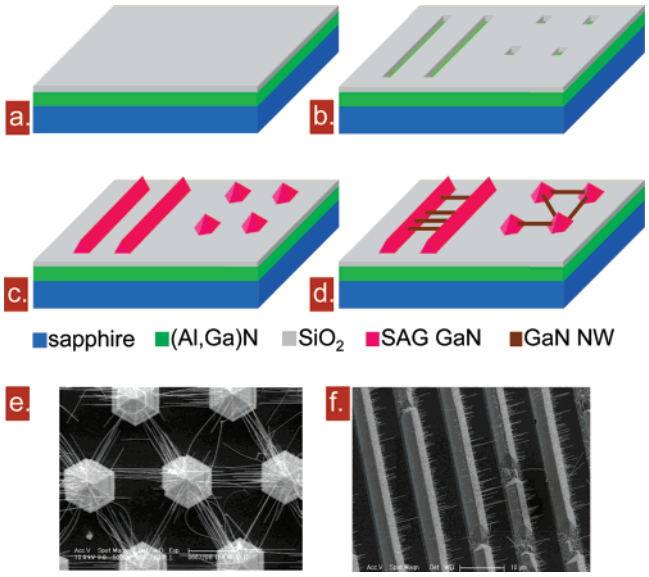

Figure 1. Schematic of SAG and VLS processes for aligned growth of GaN NWs. (a) AlN epilayer is deposited on sapphire substrate, followed by PECVD deposition of SiO_2. (b) Stripe patterns are then etched into the oxide layer. (c) GaN SAG is then carried out, followed by (d) catalyst deposition, and consequent VLS nanowire growth. (e) GaN NW network synthesized on hexagonal pyramidal mesas. (f) Arrays of GaN NWs grown on parallel *a*-axis stripes of GaN SAG mesas.

and ammonia (NH_3) were used as the precursors for Ga, Al, and N, respectively. A 100 nm thick SiO_2 layer was deposited by PECVD, followed by photolithography to form stripe or dot patterns in the oxide (Figure 1b). The stripe patterns were aligned along either $\langle 11\bar{2}0\rangle$ or $\langle 10\bar{1}0\rangle$ directions. SAG growth of GaN was performed at nominally 1030 °C. Subsequent regrowth takes place preferentially within and out of the window region through lateral diffusion of reactants due to the surface inertness of the masked region.[9] Depending on the orientations and precise shapes of the window openings, the SAG growth yielded facetted crystals bound by $\{10\bar{1}1\}$, $\{11\bar{2}2\}$, and {0001} planes (Figure 1c),[10] a process described by Wulff's theorem.[11] The GaN mesas thus formed were then used as growth templates for catalytic NW growth. Several growth orientations have been reported for the VLS synthesis of single-crystalline GaN NWs such as $\langle 10\bar{1}0\rangle$ (*m*-axis),[12] $\langle 0001\rangle$ (*c*-axis),[13] and $\langle 11\bar{2}0\rangle$ (*a*-axis).[14] The multiplicity of growth directions is likely governed by the minimization of total surface and strain energies. It has been shown that arrays of vertically aligned GaN NWs can be grown along *c* and *m* axes when crystallographically compatible substrates such as (111)MgO and (100)γ-$LiAlO_2$ are chosen, respectively.[12] One of the enabling factors for the present study is that the identified stable crystallographic facets in SAG of GaN by MOCVD, including *m* and pyramidal *m* planes, coincide with the preferential growth direction of GaN NWs[15] and therefore guide the horizontal synthesis of aligned NW arrays. Ni catalyst (1.5 nm) was deposited by e-beam evaporation, followed by transferring substrate to a hot-wall chemical vapor deposition (CVD) furnace reactor. Gallium metal was used as the Ga source. The NH_3 flow was maintained between 20 and 80 sccm. Growth temperature for the VLS synthesis varies between 850 and 950 °C. It was observed that a higher growth temperature (900−950 °C) results in thicker NWs (>70 nm) oriented along $\langle 10\bar{1}1\rangle$ directions, while a lower temperature (~850 °C) leads to thinner NWs (25−65 nm) aligned horizontally along the $\langle 10\bar{1}0\rangle$ axes (shown schematically as Figure 1d).

Table 1. Summary of Nanomechanical Measurements on a Nanowire Array of 11 Elements[a]

NW name	L (μm)	d (nm)	f_{1y} (MHz)	f_{1x} (MHz)	Q	φ (deg)
NW_1	4.30	49.0	2.062	2.323	591	62.87
NW_2	2.68	46.6	4.679	5.279	542	62.90
NW_3	2.89	46.0	4.046	4.589	757	63.02
NW_4	2.98	45.1	3.771	4.32	895	63.25
NW_5	2.17	43.0	6.903	7.828	929	63.02
NW_6	2.50	44.0	5.303	6.081	867	63.28
NW_7	2.04	40.5	7.42	8.584	1008	63.48
NW_8	4.81	53.0	1.645	1.859	717	62.94
NW_9	4.66	52.5	1.756	1.975	693	62.83
NW_10	3.52	45.0	2.805	3.179	905	63.00
NW_11	6.00	57.9	1.182	1.34	400	63.01

[a] The length and diameter of the nanowires are measured by SEM imaging, the dual fundamental modes are detected by electron beam probe method. Quality factors are obtained by Lorentzian fitting to the thermomechanical resonance peak, and the facet angle is calculated by eq 3.

Examples of directed synthesis of GaN NWs prepared by a hybrid SAG-VLS procedure are shown in Figure 1e,f. Scanning electron microscopy (SEM) was performed using a FEI XL30 field-emission microscope. GaN NW networks with hexagonal pyramidal mesas interconnected by *m*-axis NWs formed in situ without any postgrowth assembly. We note that these mesas prepared by SAG can be doped to either n- or p-type, creating junction-free electrical access to NW devices.

Conventional techniques used for studying the mechanical properties of micromechanical systems (MEMS) make use of optical measurement techniques for detecting resonances. Optical detection is however unsuitable for detecting resonance frequencies of nanowires where the diameter of the wire is much below visible wavelengths. Our approach utilizes an electron beam method to detect thermomechanical resonance in horizontally aligned nanowires.[16] The nanomechanical resonances of an array of GaN nanowire cantilevers connected to a SAG mesa were measured in a modified SEM setup.[16] An electron beam was fine-focused at the edge of a selected nanowire on a sample mounted in the SEM chamber. Given that e-beam only probes the vibrational behavior projected along the beam direction, samples were rotated relative to the surface normal to reveal spatial anisotropy in resonance modes. In the angle-resolved measurement, 0° was designated to normal incidence of e-beam onto the *c*-plane GaN. A secondary electron signal was collected and passed to a spectrum analyzer. We performed measurements upon a 6 μm long nanowire with a base width of ~58 nm (nanowire 11 in Table 1). The frequency response from such a nanoresonator at 0° and 40° tilt angle is plotted in Figure 2a, and at the latter tilt angle, we observe the presence of two peaks.

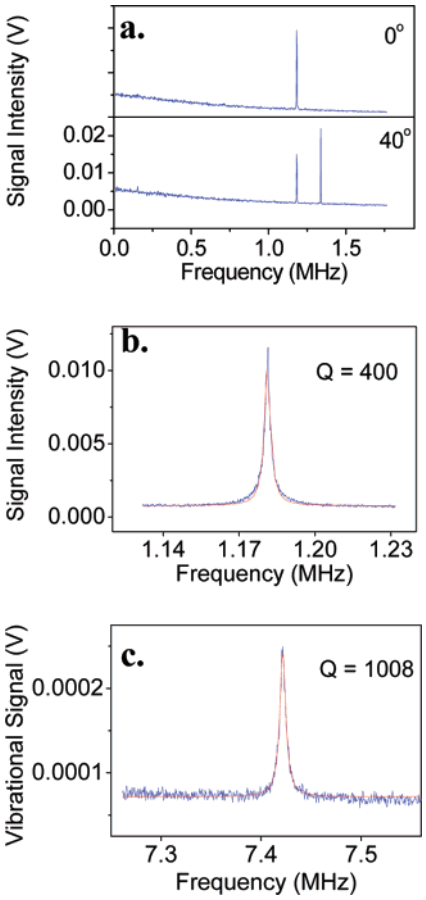

Figure 2. (a) Resonance peaks of a single NW at 0° and 40° tilt angle, respectively. (b) Lorentzian fitting of the resonant peak in (a) gives quality factor of 400. (c) High-frequency mechanical resonance measured from a 2 μm long nanowire viewed at 0° tilt angle.

The resonant frequency of a nanocantilever or nanobridge is represented by

$$f_i = B_i^2/2\pi L^2\sqrt{EI/\rho A} \tag{1}$$

where L, A, and ρ are the length, cross-sectional area, and mass density of the beam, and E and I are the Young's modulus and area moment of inertia, respectively. $B_1 = 1.875$ for the first harmonic of the cantilever resonator.[17] The appearance of two fundamental resonances is likely due to the reduced symmetry and the removal of degeneracy of orthogonal fundamental modes. The *m*-axis GaN NWs have been shown to exhibit an isosceles cross section rather than equilateral.[18]

The moment of inertia in the x and y-directions for an isosceles triangle are given by

$$I_x = bh^3/36 \tag{2a}$$

and

$$I_y = b^3h/48 \tag{2b}$$

where b and h are the base and height of the triangle, respectively, and the area of the triangle is

$$A = bh/2 \tag{2c}$$

We substitute eq 2a into eq 1 to get the resonant frequency of the mode viewed from x-axis, $f_{1x} = B_i^2/2\pi L^2\sqrt{Eh^2/18\rho}$, and eq 2b into eq 1 to get $f_{1y} = B_i^2/2\pi L^2\sqrt{Eb^2/24\rho}$, where h and b represent the height and base of the isosceles triangle in Figure 3a. The frequency ratio of the two resonances is given by

$$f_{1x}/f_{1y} = \tan\varphi/\sqrt{3} \tag{3}$$

Here φ is the isosceles base angle shown in Figure 3a. Equilateral triangle cross section has $\varphi = 60°$, in which case, only one resonance is expected. Also shown in Figure 3a is a finite element simulation of the fundamental modes with vibrational polarization along x and y directions individually. If detection is oriented along only the x- or y-axis, such as that being used in most experimental configurations, only one mode has nonzero displacement projection along the measured plane; the orthogonal mode becomes undetectable. To study this "ghost mode", we continuously rotated the nanowire along its axis in the electron microscope by manipulating the sample at the eucentric height. At 0° tilt angle, only one resonance peak is detected, however, as the tilt angle increases, the orthogonal mode becomes apparent. Figure 3c shows the nanowire resonant plots as a function of *tilt* angle for two observed orthogonal modes. The second orthogonal mode increases as the *tilt* angle is increased from 0° to 60°.

The measurement also allows simultaneous detection of the two orthogonal fundamental modes within one frequency window of a single detection circuit. This ratio is independent of mechanical properties of the nanowires, such as Young's modulus, mass density, and clamping methods, and therefore essentially free of temperature variations. For sensing applications, this frequency ratio provides direct resonant detection of cross-sectional mass accretion on a nanowire resonator and allows new methodology for real-time mass detection where the mass sensing is generally plagued by temperature drift and environmental fluctuations.

Dual mechanical resonance has been reported in literature.[19] However, because of the dispersive nature in nanowire growth involved, the dual resonances were only randomly spotted. A direct correspondence between the observed mechanical modes with the nanowire relative orientations was not established. Our unique setup enables a systematic recording of the dual resonance of GaN NWs up to a maximum rotation angle of 60°.

Table 1 represents a summary of measured results of a nanowire array of eleven nanowires. The nanowire diameters and lengths were individually measured by SEM, where the base of an isosceles triangle was taken as the diameter. The dual fundamental modes were detected by electron beam probe method. Quality factors were obtained by Lorentzian

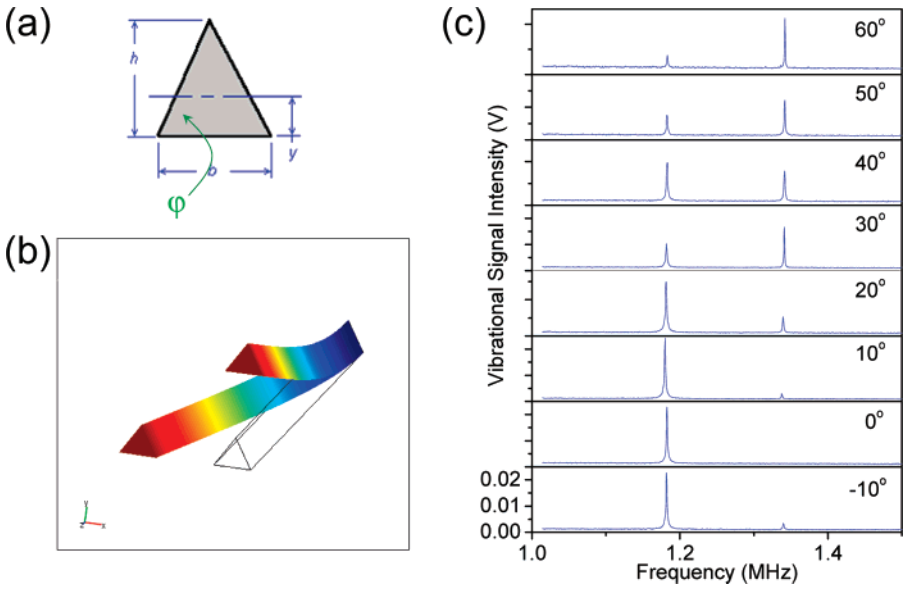

Figure 3. (a) Triangular cross-sectional area that represents the nanowire cross section. (b) Finite element simulation of two orthogonal vibration modes in the *x* and *y* directions. (c) Plot of resonance frequency of a single nanowire, only one peak (at 1.182 MHz, f_y) is observed at 0°, corresponding the *y*-axis mode; a second peak (at 1.34 MHz) appears at higher tilt angle due to vibration projected from the *x*-axis mode.

fitting to the thermomechanical resonance peak. The measurement of f_{1x} and f_{1y} enables direct determination of facet angles (φ) and Young's modulus (E) from eqs 2 and 3.

The variation of wire width due to the statistical fluctuation in high-temperature clustering of Ni represents a source of limited randomness,[21] which can be mitigated conceivably with the use of nanoparticles. This dependence is in quantitative agreement with the VLS model proposed by Givargizov:[22] $L^{1/2} = k_1 - k_2/d$, in which the coefficients k_1 and k_2 define a critical diameter, $d_C = k_2/k_1$, below d_C growth cannot commence. In this study, d_C is estimated to be approximately 25 nm. The elastic or Young's modulus (ratio of stress to strain) is an intrinsic property of a material and characterizes the stiffness of the material's interatomic forces.[23] The one-dimensional near single crystalline nature of nanowires points to lower probability of finding structural defects. Various groups have investigated the effects of Young's modulus on the diameter of nanostructures. Among these findings, there have been observed decrease in the Young's modulus on Pb and Au NWs with increasing diameters due to surface stress effects,[24] and a similar tendency was observed for ZnO NW due to surface stiffening effects arising from shortened bond lengths.[25] However, an opposite trend was observed in GaN nanowires in previous measurement by Nam et al.,[20] where the Young's modulus was found to decrease for nanowires with smaller diameters. Figure 4 represents our measured variation in Young's modulus of the GaN nanowire cantilevers with increasing nanowire length:diameter aspect ratio. Nanowire lengths vary from 2.04 to 6 μm, and the diameters vary from 40.5 to 57.9 nm (Table 1). The corresponding Young's modulus of the nanowires varies from 310 to 362 GPa, with an average value of 338 $\pm$ 21 GPa, within the range of reported theoretical and calculated values for bulk GaN to date (295−390 GPa[26,27]). Our result indicates that increasing the diameter

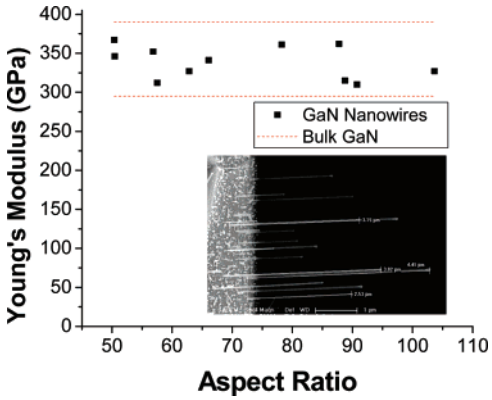

Figure 4. Variation of Young's modulus with length:thickness aspect ratio of GaN NWs. The measured NW values lie within the range of reported theoretical and experimental values for bulk GaN (295−390 GPa). Inset: SEM micrograph of the nanowire array, as measured.

of the nanowire has no effect on the Young's modulus, and this might be due to the narrow range of diameters investigated. Because the Young's modulus is a material property that depends on the atomic bonds of the material, we think that the measured Young's modulus of our nanowires lies within 5% of the bulk range due to the elasticity of the nanowires.

Quality factor (Q) characterizes the damping of a resonator. $1/Q$ is proportional to the energy loss or dissipation of the nanoresonator[28] and can be affected by both intrinsic and extrinsic mechanisms. When suspended in air, the nanoresonator is affected by air damping, while when suspended in vacuum, effects due to defects and surface states arise. NEMS measurements were carried out at 10^{-6} Torr, so measured Qs are limited by energy dissipation due to intrinsic factors. We obtained Qs between 400 and 1008 and observed an inverse dependence on the length. The underlying

mechanism remains unclear to us. Measurements upon a larger ensemble of nanowires with varying growth conditions are required to ascertain the trend with sufficient statistics.

The ratio of the two observed frequencies allows us to calculate the base angle of our nanowires. An angle of ~63.1° was consistently measured (Table 1), representing a first accurate determination of the geometrical configuration of NWs from nanomechanical rather than microscopical measurements. We note that, in the SAG growth of GaN from *m*-axis stripes, the triangular mesas are typically bound by $(000\bar{1})$ and two $\{11\bar{2}2\}$ planes, thus requiring an inclined angle of 58.4° from crystallographic consideration.[29] However, we also note that *m*-axis SAG stripes with varying facet angles (~58°−72°) have been observed;[30] the formation of $\{11\bar{2}n\}$ facets, where $n \approx 1-2.5$, was speculated due to the atomistic surface reconstruction that alters the energetics during growth. The presence of nanoscale faceting on the NW sidewalls[31] can conceivably alter the energetics and affect the base angle.

In the above analysis, the nanowires are assumed to have isosceles cross section. This hypothesis was confirmed with two independent measurements: (a) SEM imaging while sample is tilted from −60° to 60°, and (b) measurement of dual resonances while sample tilt is changed from −60° to 60°. Upon reversal of tilt angles, we obtained similar values in both wire diameter and resonant amplitude, indicating image reversal symmetry along the sample normal.

In summary, we report the epitaxial growth of arrays of GaN NWs and interconnected networks. Highly oriented nanowire arrays and networks are obtained through a hybrid approach that includes both top-down selective area growth and bottom-up catalytic synthesis. Nanomechanical characterizations are performed upon individual nanowires. For all the wires we measured, we obtain consistent Young's modulus close to that of the predicted bulk value in GaN. Precise value of the nanowire facet angle is obtained by measuring the ratio of fundamental resonances in orthogonal planes of the nanowire.

Acknowledgment. H.X.T. acknowledges support from Yale University faculty startup funds and support from Caltech's NEMS (Roukes) group and Caltech's Kavli Nanoscience Institute at early stage of this work.

References

(1) Huang, Y.; Duan, X.; Lieber, C. M. *Pure Appl. Chem.* **2004**, *76*, 2051.
(2) Cui, Y.; Wei, Q.; Park, H.; Lieber, C. M. *Science* **2001**, *293*, 1289.
(3) Craighead, H. G. *Science* **2000**, *290*, 1532.
(4) Ekinci, K. L.; Huang, X. M. H.; Roukes, M. L. *Appl. Phys. Lett.* **2004**, *84*, 4469.
(5) Yang, Y. T.; Callegari, C.; Feng, X. L.; Ekinci, K. L.; Roukes, M. L. *Nano Lett.* **2006**, *6*, 583.
(6) Huang, X. M. H.; Zorman, C. Z.; Mehregany, M.; Roukes, M. L. *Nature* **2003**, *421*, 496.
(7) Carr, D. W.; Evoy, S.; Sekaric, L.; Craighead, H. G.; Parpia, J. M. *Appl. Phys. Lett.* **1999**, *75*, 920.
(8) Gherasimova, M.; Cui, G.; Ren, Z.; Su, J.; Wang, X.-L.; Han, J.; Higashimine, K.; Otsuka, N. *J. Appl. Phys.* **2004**, *95*, 2921.
(9) Mitchell, C. C.; Coltrin, M. E.; Han, J. *J. Cryst. Growth* **2001**, *222*, 144.
(10) We note that, at growth conditions conducive to pronounced lateral growth, prism planes such as {10*1*0} begin to emerge. While such vertical sidewalls do support the growth of *m*-axis GaN NWs, they present difficulty in applying catalyst and are subsequently avoided.
(11) Du, D.; Srolovitz, D. J.; Coltrin, M. E.; Mitchell, C. C. *Phys. Rev. Lett.* **2005**, *95*, 155503.
(12) Duan, X.; Lieber, C. M. *J. Am. Chem. Soc.* **2000**, *122*, 188.
(13) Kuykendall, T.; Pauzauskie, P. J.; Zhang, Y.; Goldberger, J.; Sirbuly, D.; Denlinger, J.; Yang, P. *Nat. Mater.* **2004**, *3*, 524.
(14) Gradečak, S.; Qian, F.; Li, Y.; Park, H. G.; Lieber, C. M. *Appl. Phys. Lett.* **2005**, *87*, 173111.
(15) Kim, K.; Henry, T.; Cui, G.; Han, J.; Song, Y.-K.; Nurmikko, A. V.; Tang, H. X. *Phys. Status Solidi B* **2007**, *244*, 1810.
(16) Buks, E.; Roukes, M. L. *Europhys. Lett.* **2001**, *54*, 220.
(17) Meirovich, L. *Element of Vibration Analysis*; McGraw-Hill: New York, 1986.
(18) Kuykendall, T.; Pauzauskie, Lee, S. K.; Zhang, Y. F.; Goldberger, J.; Yang, P. D. *Nano Lett.* **2003**, *3*, 1063.
(19) Bai, X. D.; Gao, P. X.; Wang, Z. L.; Wang, E. G. *Appl. Phys. Lett.* **2003**, *82*, 4806.
(20) Nam, C.-Y.; Jaroenapibal, P.; Tham, D.; Luzzi, D.; Evoy, S.; Fischer, J. E. *Nano Lett.* **2006**, *6*, 153.
(21) Family, F.; Meakin, P. *Phys. Rev. Lett.* **1988**, *61*, 428.
(22) Givargizov, E. I. *J. Cryst. Growth* **1975**, *31*, 20.
(23) Liu, C. *Foundations of MEMS*; Illinois ECE Series; Prentice Hall: Upper Saddle River, NJ, 2006.
(24) Cuenot, S.; Frétigny, C.; Demoustier-Champagne, S.; Nysten, B. *Phys. Rev. B* **2004**, *69*, 165410.
(25) Chen, C. Q.; Shi, Y.; Zhang, Y. S.; Zhu, J.; Yan, Y. J. *Phys. Rev. Lett.* **2006**, *96*, 075505.
(26) Nowak, R.; Pessa, M.; Suganuma, M.; Leszczynski, M., Grzegory, I.; Porowski, S.; Yoshida, F. *Appl. Phys. Lett.* **1999**, *75*, 2070.
(27) Schwartz, R. B.; Khachaturyan, K.; Weber, E. R. *Appl. Phys. Lett.* **1997**, *70*, 1122.
(28) Cleland, A. *Foundations of Nanomechanics: From Solid-State Theory to Device Applications*; Springer-Verlag: Berlin, 2003.
(29) Hiramatsu, K.; Nishiyama, K.; Motogaito, A.; Miyake, H.; Iyechika, Y.; Maeda, T. *Phys. Status Solidi A* **1999**, *176*, 535.
(30) Marchand, H.; Ibbetson, J. P.; Fini, P. T.; Keller, S.; DenBaars, S. P.; Speck, J. S.; Mishra, U. K. *J. Cryst. Growth* **1998**, *195*, 328.
(31) Ross, F. M.; Tersoff, J.; Reuter, M. C. *Phys. Rev. Lett.* **2005**, *95*, 146104.

NL071530X